Transverse hot-electron focusing

R. I. Hornsey, J. R. A. Cleaver, and H. Ahmed
Microelectronics Research Centre, Cavendish Laboratory, University of Cambridge, Cambridge CB3 0HE, United Kingdom
(Received 9 August 1993)

Transverse electron focusing is reported for hot electrons. Differential transresistance measurements show anomalous behavior at high electron energies. Corresponding dc electron focusing data reveal that the differential characteristics arise from the electron energy dependences of the mean free path and specularity coefficient. The variation of mean free path with energy is derived from the experimental data.

The use of ballistic electrons in a high-mobility two-dimensional electron gas (2DEG) is now well established as a means of exploring mesoscopic device behavior. These electrons experience no impurity scattering over a distance characterized by their mean free path (mfp), which can be >10 μm. Usually, care is taken to ensure that measurement signals do not excite the electrons significantly above their Fermi energy E_F. However, interesting studies have been carried out to investigate the scattering properties of electrons with energies in excess of E_F, so-called hot electrons. Sivan, Heiblum, and Umbach[1] reported the observation of ballistic hot electrons with a mfp of ~ 2 μm (cf. a cold-electron mfp of 4.5 μm) when the excess energy was less than 36 meV, the longitudinal-optical (LO) phonon emission energy. This contrasted with a theoretically expected value of about 0.2 μm. Ballistic transport of hot electrons over a distance greater than 2 μm has also been reported elsewhere.[2]

A convenient method for studying hot-electron transport is transverse electron focusing (TEF).[2,3] The device, shown in the inset of Fig. 1(b), consists of adjacent injector and collector constrictions in the 2DEG. With an applied magnetic field, electrons from the injector can be focused into the collector, giving transresistance peaks when $nR_{\rm cycl}=S/2$, where n is an integer, $R_{\rm cycl}$ is the cyclotron radius, and S is the separation of injector and collector. Because $R_{\rm cycl}$ is dependent on the electron energy [$R_{\rm cycl}=\sqrt{(2m^*E)}/eB$, where m^* is the effective mass of the electron, E is the energy, e is the electronic charge, and B is the magnetic field], this technique enables the electron energies to be derived from the magnetic fields at which the peaks occur.

Independent data presented by Williamson *et al.*[2] and by Laikhtman *et al.*[3] revealed anomalous changes in the TEF characteristics when the electron energy was increased above E_F. As expected, the resistance peaks initially moved towards higher magnetic fields but, beyond a certain energy, another set of peaks appeared to develop. These new peaks became dominant at high electron energies and were almost midway between the low-energy peak positions. Laikhtman *et al.*[3] attributed the changes in the TEF characteristics to the injection of high-energy electrons into the second subband of the 2DEG, thereby causing peaks at different positions. The long hot-electron mfp implied by these data was thought to result from reduced electron scattering in the higher subband. In the present paper, we report a TEF experiment which yields similar results. It will be demonstrated, however, that these effects, measured with an ac differential technique, can be accounted for by changes in the dc TEF

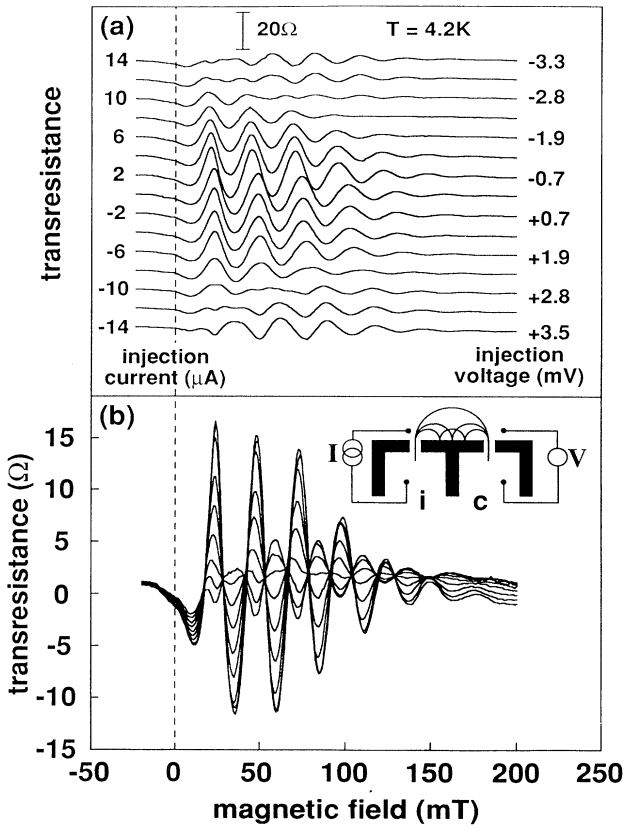

FIG. 1. Differential TEF magnetotransresistance for different injection currents; for negative and positive currents, the injector acts as an electron source and sink, respectively. (a) Characteristics for ± 14 μA, with corresponding accelerating potentials (see text); curves offset. (b) Characteristics for several positive values of injection current up to 14 μA; curves overlaid. (Inset: device schematic showing transresistance measurement; *i* denotes the injector and *c*, the collector.)

characteristics, and do not require an explanation based on higher-subband transport. Finally, the variation of mfp with electron energy is derived from the dc data.

These devices were fabricated by Si ion implantation at an energy of 120 keV and a dose of 10^{13} cm^{-2} into a 580-nm-deep GaAs/$Al_xGa_{1-x}As$ heterojunction through a patterned polymethylmethacrylate mask. The implants were not annealed and, therefore, insulating areas defining the injector and collector structure were created in the 2DEG by channeled ions. Details of the fabrication are reported elsewhere.[4] For unimplanted samples, the mobility and carrier concentration after illumination were 3.1×10^6 cm^2/V s and 5.3×10^{11} cm^{-2}, respectively, at 4.2 K. TEF devices were fabricated with an injector-to-collector separation of 11 μm, giving an electron path length of 17.3 μm (cf. a mfp >30 μm), and the defined constriction widths were 1 μm.

Measurements were performed using standard low-frequency ac lock-in differential magnetoresistance techniques, using the four-terminal configuration shown in the inset of Fig. 1(b). The 100 nA ac-measurement current was superimposed on a variable dc current I, which is quoted as a conventional current from the injector. It should be noted that the 1-μm-wide injector supports >30 transverse modes so it is not meaningful to consider the injection voltage and current independently.

Figure 1(a) shows TEF results, displaying a change of peak structure for $|I|\geq\sim8$ μA similar to that reported elsewhere.[2,3] A different device, with an injector width of 0.5 μm, demonstrates the same effect at about half this current. Injection voltages corresponding to the injection currents have been estimated by measuring the two-terminal voltage-current characteristics of the injector and subtracting the voltage drop across the Ohmic contacts. The ratios of the electron energies determined from the TEF peaks at low currents to those expected from the injector voltage drops are >0.98. Previous data for split-gate devices gave values[2,3] of 0.68 and 0.82, which Laikhtman *et al.*[3] attributed to $\mathbf{E}\times\mathbf{B}$ drift caused by the biased-surface gates. Since there are no surface gates in the present case, the near-unity coefficients observed here are to be expected.

Overlaid plots in Fig. 1(b) show that the ac TEF characteristics at high injection currents are in direct antiphase with those at low currents; the nodes at each half cycle are very clear. The decreasing transresistances at successive peaks arise from the nonunity specularity coefficient of the electron reflection at the ion-implanted boundary. Average specularities of ~0.6 are typical for such devices.[4] Data for larger current intervals are shown for another, nominally identical, device in Fig. 2. It is seen that the transition is again well developed at about 10 μA and the antiphase resistance peaks reach a maximum amplitude at ~20 μA before dying away with no further phase changes.

The data given in Figs. 1 and 2 enable the second-subband hypothesis proposed by Laikhtman *et al.*[3] to be reexamined. Regardless of the subband in which the electrons are transported, the TEF peaks should be found at magnetic fields which are integral multiples of the value for the first peak. However, it is apparent from the

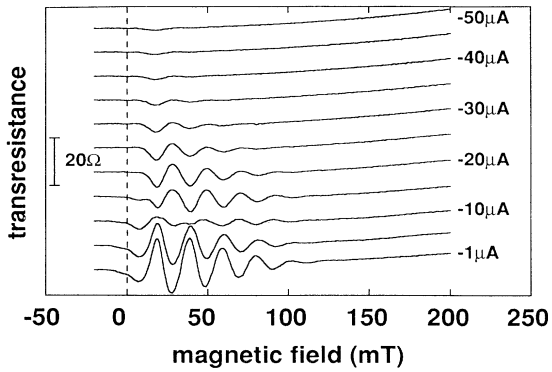

FIG. 2. Differential TEF magnetotransresistance for larger injection currents, showing the antiphase transition and subsequent dying out of the focusing characteristics.

figures that this is not the case when $|I|>10$ μA. Moreover, the transition to second-subband transport should be exhibited simultaneously by all peaks, whereas Fig. 1(a) shows that the change occurs progressively, starting with the high-field peaks. The hypothesis that electrons are injected into higher subbands of the 2DEG is not consistent with these observations. The discussion by Williamson *et al.*[2] concerns an injector with one occupied one-dimensional subband and is therefore not applicable to the 1-μm-wide constriction considered here.

We note that the resistance measured by an ac differential technique is the local gradient of the device V-I curve. Usually, the measurement is made near the origin, where the device is assumed to have a linear characteristic. Adding a dc value to the ac measurement signal means that the point at which the local gradient is measured is offset from the origin. If the device characteristics are nonlinear, $dV/dI\neq V/I$, so the differential resistance measurement can be misleading. Accordingly, dc V-I curves for the four-terminal configuration have been measured [Fig. 3(a)] at values of the magnetic field corresponding to the peaks and valleys in Fig. 2. These curves are highly nonlinear and their derivatives give the variation of differential resistance with current at these magnetic fields (cf. Fig. 2). It should also be noted that the changing signs of the gradients in Fig. 3 give rise immediately to the antiphase structure of the differential TEF characteristics.

To determine the reasons for the nonlinearity of the V-I curves, a series of dc TEF characteristics has been measured. For each curve, a constant current was passed through the injector and the dc collector voltage was recorded as a function of B [Fig. 3(b)]. The form of the curves for currents in opposite directions is explained as follows: for the negative currents, electrons are sourced from the injector as usual so that, when the focusing criterion is met, electrons enter the collector and a negative voltage is recorded (dividing by the negative injection current gives the familiar resistance peaks). At first sight, it is surprising that a TEF characteristic is obtained also for positive currents, when the injector acts as an electron sink; however, consider the focused condition, when $nR_{\rm cycl}=S/2$ (the case for $n=1$ is shown in the inset of

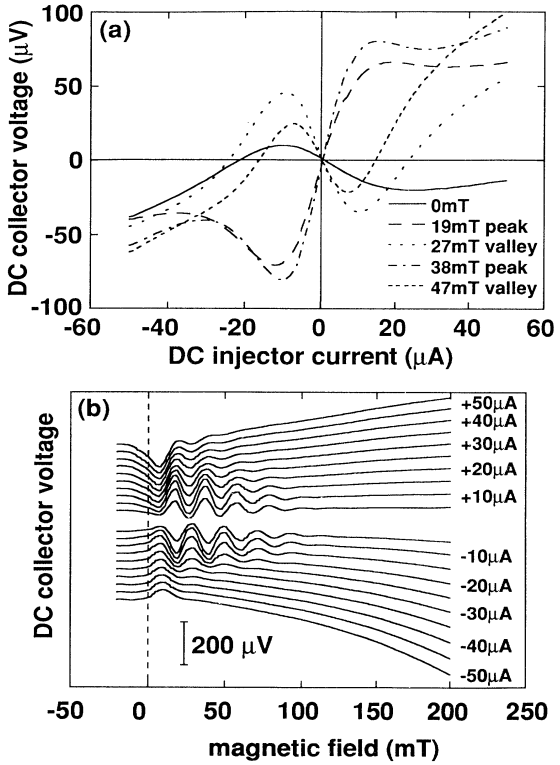

FIG. 3. dc measurements of TEF. (a) Voltage-current curves for various magnetic fields corresponding to the peaks and valleys in Fig. 2. (b) dc magnetovoltage data for various injector currents; curves offset.

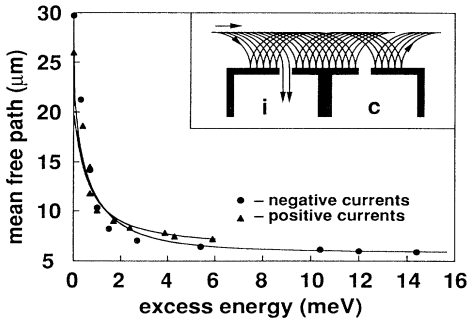

FIG. 4. Variation of electron mfp with energy derived from the experimental data in Fig. 3; solid lines are to guide the eye (inset: schematic of skipping orbits when injector acts as a current sink).

Fig. 4). Electrons approach the injector from the left in clockwise skipping orbits along the front of the device. None of these electrons can enter the collector because they are trapped by the injector before they reach it. Therefore, the focused condition is always represented by a positive voltage (fewer electrons) on the collector, the reverse of the negative current case. Because the effect of electron heating is the same in both cases, the electrons are focused at higher fields for higher currents, irrespective of the current direction. This confirms that the injected electrons are heated above E_F even though their actual energy may not necessarily be equal to that expected from the full applied potential. In the dc measurements, there are no phase changes at the higher currents and no evidence for second-subband transport.

Returning to the V-I curves in Fig. 3(a) in the light of the dc TEF data, we suggest that the characteristics arise from the combination of two effects; the transport properties of the hot electrons in the 2DEG and their interaction with the ion-implanted boundary. The total path length of the collected electrons is independent of the number of boundary reflections and any effect of the transport is therefore common to the V-I curves at the magnetic fields of all peaks and valleys. However, the first peak characteristic represents the only electron trajectory which has not been reflected from the boundary so it alone is unaffected by boundary scattering. Other peaks and valleys arise from the electron trajectories that are affected by the properties of hot-electron transport as well as by boundary scattering. At high fields, the peak shifts due to electron heating and the background Hall voltage also become important.

Considering the boundary interactions first, it is clear from Fig. 3(b) that fewer of the TEF peaks are resolvable at higher currents. This is consistent with energy dependence of the specularity coefficient of the boundary scattering. The background Hall component on these curves makes reliable determination of the specularity difficult but, from best estimates, it varies approximately linearly with the current, from ~ 0.6 at $I=0$ to ~ 0.2–0.3 at $|I|=50\,\mu$A. It is this variation of specularity that causes the progressive change in the differential characteristics described in connection with Fig. 1.

It is proposed that the nonlinearity of the V-I characteristic for the first peak (with no boundary scattering) is the result of a strong energy dependence of the electron mfp. We assume that the collector voltage is proportional to the number of electrons collected per unit time which, for a mfp constant at the cold-electron value λ, would also be proportional to I (ignoring small changes due to the movement of the peak). This linear relationship is apparent near the origin of the V-I curve [Fig. 3(a)]. A smaller proportion of the hot electrons reaches the collector because their mfp is shorter than λ. The proportion that do, $r_{\rm hot}$, is therefore $V(I)/aI$, where $V(I)$ is the measured V-I dependence and a is the gradient of the V-I curve at the origin. At a distance L from the injector ($L=\pi S/2$ here), the number of cold electrons per unit time is proportional to $I\exp(-L/\lambda)$. A similar expression holds for the hot electrons, so now $r_{\rm hot}=\exp[L/\lambda-L/\lambda(I)]$, where $\lambda(I)$ is the hot-electron mfp. Equating the expressions for $r_{\rm hot}$, and rearranging gives

$$\lambda(I)=\left[\frac{1}{\lambda}-\frac{1}{L}\ln\frac{V(I)}{aI}\right]^{-1}.$$

For this device, $\lambda=31\ \mu$m and $V(I)$ and a are derived from Fig. 3(a). The variation of mfp with excess electron energy (relative to that calculated from TEF data at ± 5

μA, $\sim$13 meV) is shown in Fig. 4, where the energies have been calculated as a function of I from the positions of the dc TEF peaks in Fig. 3(b). The shape of this curve and the relative values of the mfp are similar to those calculated by das Sarma.[5] The 2D calculation showed that, for electron energies below the LO phonon emission energy (36 meV), the inelastic scattering of hot electrons is mainly due to the excitation of electron-hole pairs within the 2DEG.

In conclusion, we have presented extensive data for differential magnetotransresistance measurements of transverse hot-electron focusing. These show that a significant change in the characteristics occurs when the dc offset current exceeds about 10 μA. It is shown that the differential data are related to dc magnetovoltage curves, which are interpreted in relatively simple terms. Hot-electron mean free paths, as a function of electron energy, are derived from the dc data; the values are consistent with a model of scattering due to the excitation of electron-hole pairs.

The authors wish to thank R. J. Blaikie, B. Alphenaar, A. M. Marsh, and S. G. Ingram for many stimulating discussions.

[1]U. Sivan, M. Heiblum, and C. P. Umbach, Phys. Rev. Lett. **63**, 992 (1989).

[2]J. G. Williamson, H. van Houten, C. W. J. Beenakker, M. E. I. Broekaart, L. I. A. Spendeler, B. J. van Wees, and C. T. Foxon, Phys. Rev. B **41**, 1207 (1990); Surf. Sci. **229**, 303 (1990).

[3]B. Laikhtman, U. Sivan, A. Yacoby, C. P. Umbach, M. Heiblum, J. A. Kash, and H. Shtrikman, Phys. Rev. Lett. **65**, 2181 (1990).

[4]R. I. Hornsey, J. R. A. Cleaver, and H. Ahmed, J. Appl. Phys. **73**, 3203 (1993).

[5]S. das Sarma, in *Hot Carriers in Semiconductor Nanostructures,* edited by J. Shah (Academic, New York, 1992).